2011 American Control Conference
on O'Farrell Street, San Francisco, CA, USA
June 29 - July 01, 2011

Design for Dynamic Performance: Application to an Air Separation Unit

Yanan Cao, Christopher L.E. Swartz and Michael Baldea

Abstract— **The significant effect that the design of a plant can have on its dynamic performance has led to methodologies for systemic analysis of the interaction between design and control, and for inclusion of dynamic performance considerations in plant design. In this paper, an optimization-based approach is presented for identifying design characteristics that limit plant agility in the face of production demand and electricity price changes. Responding optimally to such variation could have a significant impact on plant economics and operational efficiency. The problem formulation is described, and its efficacy demonstrated through application to a case study based on an industrial nitrogen production plant. Conclusions are drawn, and avenues for future research identified.**

I. INTRODUCTION

The design of a plant can have a significant effect its dynamic performance. A plant with poor dynamic performance characteristics may result in failure to meet product quality specifications, safety and environmental constraints, and expected economic performance. The interaction between process design and dynamic performance has led to several research studies toward systematic analysis of design limitations to control performance, and incorporation of dynamic performance considerations within the plant design framework [1][2][3].

Dynamic optimization provides a useful framework for the assessment of control performance limitations. Approaches include open-loop formulations [4][5], controller parametrization to provide performance limits for linear feedback control [6], and inclusion of specific controller types, such as PI control [7]. Performance metrics include economic [7], set-point tracking [6][4] and speed of response [5]. In optimization-based approaches to simultaneous plant and control system design, dynamic performance is accounted for implicitly through an economic objective function and path constraints on the input and response trajectories [8][9][10].

In this paper, we consider dynamic performance limitations in an air separation plant. Cryogenic separation of air is a widely used technology for producing high purity nitrogen, oxygen and argon for use in a number of market sectors including the steel, semiconductor, medical, pulp and paper, and food processing industries. It is a large consumer of electrical energy, with the consumption of electricity by gas producers in the United States exceeding $700 million/year [11]. Air separation units are subject to variation in customer demand as well as electricity price fluctuations; responding optimally to these changes, which are often frequent, would have significant impact on plant economics and operational efficiency.

This paper presents an approach toward identifying design characteristics of air separation plants that limit agility. It involves solution of two optimization problems in sequence. In the first, the target steady-state operating point is determined based on economics, more specifically, on the basis of electricity consumption, gas nitrogen (GN_2) sales and vaporization costs of pre-stored liquid nitrogen. In the second, the optimal transition from the current to target steady-state is determined to minimize a measure of transition time. Both optimization problems are subject to operating constraints that include product quality, flooding and compressor surge constraints. In the following sections we describe the dynamic model developed, optimization problem formulations, preliminary results, and conclude with a summary of key findings and future research directions.

II. MATHEMATICAL MODEL OF AIR SEPARATION UNIT

To motivate this study, we will focus on the nitrogen production plant, a simplified schematic of which is shown in Fig. 1 [11]. The intake air from the atmosphere is first compressed through a multi-stage compressor and then introduced to an adsorber or other purification units to remove impurities such as carbon dioxide and water. The treated air feed is cooled against the returning gas product stream and waste stream from the distillation column in a multi-path heat exchanger. A portion of the air feed is withdrawn from an intermediate point of the heat exchanger and goes through a turbine for additional cooling prior to being introduced to the column. The air feed, entering at the bottom of the column, is distilled into a high purity nitrogen stream, which leaves at the top, and a liquid crude oxygen stream, which accumulates at the bottom. Part of the overhead stream is withdrawn as the gas product while the rest is sent to the integrated reboiler/condenser to exchange heat with the crude oxygen stream drawn from the bottom to produce the reflux stream and the liquid nitrogen product.

In order to develop a rigorous model for the nitrogen plant to capture the plant constraints and adequately represent its nonlinear nature, individual models were developed first and then assembled in accordance with the plant configuration. The proposed integrated plant model includes both first principles and empirical models. In this study, the following components were modeled:

- distillation column with integrated reboiler/condenser
- primary heat exchanger

Y. Cao and Christopher L.E. Swartz are with Faculty of Chemical Engineering, McMaster University, 1280 Main St W, Hamilton ON L8S 4L7, Canada swartzc@mcmaster.ca

Michael Baldea is with Advanced Control and Operations Research, Praxair Technology Center, Tonawanda, NY 14150, USA

978-1-4577-0079-8/11/$26.00 ©2011 AACC

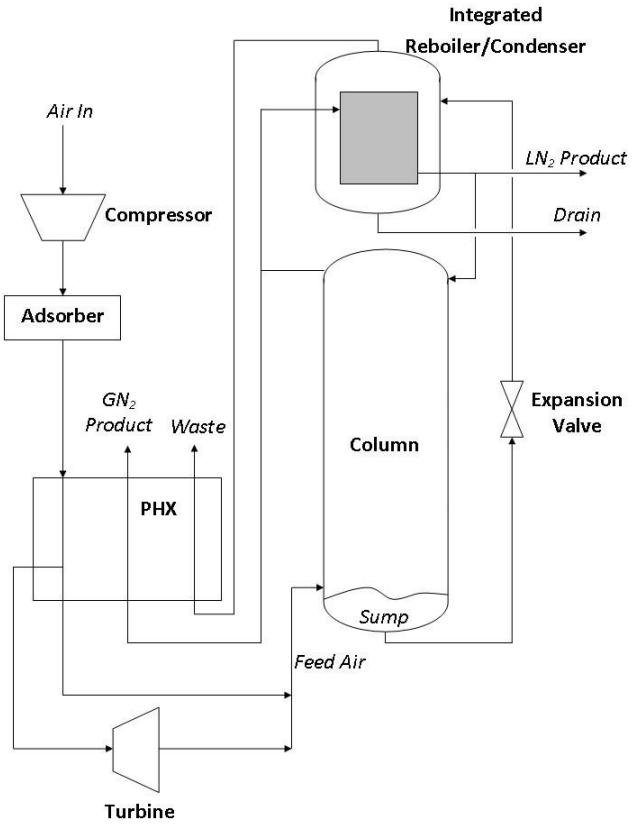

Fig. 1. Nitrogen plant process diagram [11]. LN_2 = Liquid Nitrogen; GN_2 = Gas Nitrogen; PHX = Primary Heat Exchanger.

- compressor
- turbine.

A. Distillation Model

The dynamic distillation model follows a typical approach as documented in many studies on distillation columns, such as Roffel et al. [12], Bansal et al. [13] and Miller et al. [14]. In this study, component material and energy balances are expressed as differential equations at each column tray. Vapor-liquid phase equilibrium, thermodynamic and hydraulic models are in the form of algebraic equations. This results in the general column model being formulated as a differential algebraic equation (DAE) system. Some features of the model are:

- Ternary column with components: N_2, O_2 and Ar.
- Tray hydraulics are represented by the Francis Weir equation [15].
- Vapor-liquid phase equilibrium is captured by the Modified Raoult's Law and the Antoine equation [16].
- The Margules equation is implemented for estimating activity coefficients [17].
- Murphree tray efficiencies are employed.
- The vapor velocity and the flooding velocity are estimated at each tray [13][18].

The integrated reboiler/condenser (IRC) includes two submodels: one for the condenser side and another for the reboiler side. It was assumed that there is no heat loss between the reboiler and the condenser [19]. For the condenser model, it was assumed that the condenser side has neither material nor energy holdup [19]. The vapor drawn into the condenser would go through a phase change and leave the condenser as a saturated liquid. The reboiler is modeled in a similar way as the column tray, except that a steady-state energy balance is used, derived in a similar manner as in Roffel et al. [12]. The flow rate of the bottom liquid and the drain are controlled using two proportional-integral level controllers.

B. Primary Heat Exchanger (PHX) Model

The primary heat exchanger is modeled following a similar approach as in Miller et al. [14]; however, in the present configuration there are three counter-current processing streams instead of two. Changes in metal wall temperature as well as the process stream temperatures with respect to time are captured by using differential equations. Algebraic equations arise in the calculation of the thermal properties of the streams. The distributed nature of the PHX is approximated by dividing it into a number of segments, with the assumption that in each small segment, the fluid is well mixed. The number of segments chosen has to be large enough to avoid the occurrence of temperature crossover. Pressure drop of the processing streams across the heat exchanger is included.

C. Compressor and Turbine Models

Models for the compressor and the turbine comprise systems of algebraic equations. The multi-stage compressor was modeled using available compressor maps, coupled with use of polytropic efficiency relationships. The turbine model was developed in a similar manner.

D. Composite Plant Model

After assembling the individual models in accordance with the plant configuration, a parameter estimation step was conducted to reconcile the model with available plant data. Estimated parameters include heat transfer coefficients and tray efficiencies. The resulting plant model system has four degrees of freedom: (1) air feed flow rate to the system, (2) LN_2 production or reflux rate, (3) liquid or vapor air feed flow rate to the column, (4) gas rate from top tray to PHX or IRC.

III. OPTIMIZATION PROBLEM FORMULATION

In this phase of the study, a base case design is specified and limits to control performance in response to variations in electricity price and production demand identified via optimization in a two-tiered approach. First, a steady-state optimization problem is solved to determine an economically optimal target operating point. This is followed by dynamic optimization to determine the optimal transition to the new steady-state.

A. Steady-state Optimization

We remark first that the product demand can be met by gas nitrogen produced, supplemented by evaporation of pre-stored liquid nitrogen. The steady-state optimization takes the following form:

$$\max_{\mathbf{u},F_{evap}} \Phi_{ss} = C_{\mathrm{GN}_2}(F_{\mathrm{GN}_2,prod} + F_{evap}) - (C_{comp}W_p + C_{evap}F_{evap}) \quad (1)$$

subject to

$$\mathbf{f}(\dot{\mathbf{x}} = \mathbf{0}, \mathbf{x}, \mathbf{z}, \mathbf{u}, \mathbf{p}) = \mathbf{0} \quad (2)$$

$$\mathbf{g}(\mathbf{x}, \mathbf{z}, \mathbf{u}, \mathbf{p}) = \mathbf{0} \quad (3)$$

$$\mathbf{h}(\mathbf{x}, \mathbf{z}, \mathbf{u}, \mathbf{p}) \leq \mathbf{0} \quad (4)$$

where $\mathbf{x}$ is a vector of differential states; $\mathbf{z}$ is a vector of algebraic states; $\mathbf{u}$ is a vector of control inputs; $\mathbf{p}$ is a vector of parameters; $F_{\mathrm{GN}_2,prod}$ is the flow rate of gas nitrogen produced; F_{evap} is the flow rate of evaporated liquid nitrogen; W_p is the power consumption of the compressor; C_{GN_2} is the sales price of gas nitrogen; and C_{comp} and C_{evap} are the costs associated with compression and evaporation respectively. $\mathbf{f}$ and $\mathbf{g}$ comprise the DAE plant model equations, and $\mathbf{h}$ includes variables bounds, operational constraints (such as flooding and compressor surge constraints), production specification constraints (such as demand specification and product purity constraints), and constraints required in the model (such as bubble point pressure constraint on liquid air feed).

By solving this optimization problem, an economically optimal steady-state operating point is obtained, which is then supplied to the dynamic optimization formulation.

B. Dynamic Optimization

The purpose of the dynamic optimization is to determine a set of input trajectories that drive the plant to the target steady-state operating point (and remain there) as rapidly as possible, subject to path constraints that define a feasible operating window. This objective is represented in this study through the following dynamic optimization problem:

$$\min_{\mathbf{u}(t),t_f} \Phi = t_f \left\{ \int_{t_0}^{t_f} \left(1 - \frac{F_{\mathrm{GN}_2,prod}}{F^*_{\mathrm{GN}_2,prod}}\right)^2 dt + \sum_{i=1}^{N_u} w_i \left[1 - \frac{u_i(t_f)}{u_i^*}\right]^2 \right\} \quad (5)$$

subject to

$$\mathbf{f}(\dot{\mathbf{x}}(t), \mathbf{x}(t), \mathbf{z}(t), \mathbf{u}(t), \mathbf{p}, t) = \mathbf{0} \quad (6)$$

$$\mathbf{g}(\mathbf{x}(t), \mathbf{z}(t), \mathbf{u}(t), \mathbf{p}, t) = \mathbf{0} \quad (7)$$

$$\mathbf{h}(\mathbf{x}(t), \mathbf{z}(t), \mathbf{u}(t), \mathbf{p}, t) \leq \mathbf{0} \quad (8)$$

$$t_0 \leq t \leq t_f \quad (9)$$

where w_i are weights associated with each input variable; $F^*_{\mathrm{GN}_2,prod}$ and u_i^* are the target gas nitrogen product flow rate and manipulated inputs determined in the steady-state optimization; and N_u is the number of manipulated inputs.

Except for the demand satisfaction constraint, all the constraints considered in Tier 1 are translated as path constraints, and are handled by a combination of interior-point constraints and end-point inequality constraints, which track the accumulated squared constraint violations over the time horizon. However, the value of maximum allowable impurity level during the transition is relaxed to a lower safety margin than that incorporated in the steady-state impurity specification. In addition, to pin down the final value of the inputs, we require:

$$-\varepsilon_i \leq 1 - \frac{u_i(t_f)}{u_i^*} \leq \varepsilon_i. \quad (10)$$

Reaching the desired operating condition is thus a hard constraint in the optimization problem and the last term in Eqn. 5 is mainly for improving the numerical performance of the problem. The system has to achieve steady-state at t_f, imposed through:

$$\sum_{i=1}^{no.\ comp.} \left| \frac{dm_{1,i}(t_f)}{dt} \right| \leq \varepsilon_{ss}, \quad (11)$$

where the $m_{1,i}$ are the top tray component holdups. Finally, the desired production rate has to be satisfied at t_f:

$$-\varepsilon_{prod} \leq 1 - \frac{F_{\mathrm{GN}_2,prod}(t_f)}{F^*_{\mathrm{GN}_2,prod}} \leq \varepsilon_{prod}. \quad (12)$$

In the above, ε_i, ε_{ss} and ε_{prod} are specified tolerances.

C. Control Vector Parameterizations

Control vector parametrization is used to specify the control inputs [20], using piecewise linear profiles with continuity at the control interval boundaries as in White et al. [5]. This adds the following differential equations to the system:

$$\frac{du_i}{dt} = a_{i,j}, \quad t \in [t_j, t_j + \delta_j] \quad (13)$$

where $a_{i,j}$ is the slope of the control trajectory of input i in control interval j; and t_j and δ_j are the starting time and duration of control interval j respectively. The decision

variables in this case are the slopes of the input variables in each control interval. The duration time of each control interval can be specified or optimized.

D. Optimization Platform

The commercial software package gPROMS 3.3.1 is used for simulation and optimization. The solver for DAEs in gPROMS is DASOLV, which uses backward differentiation formulae and follows the predictor-corrector approach. The solver selected for optimization is CVP_SS, which implements a single-shooting dynamic optimization algorithm, while SRQPD, employing a sequential quadratic programming method, is used as the NLP solver [21].

IV. RESULTS AND DISCUSSION

Results following the proposed approach are presented in this section. Scenarios evaluated include both demand changes and electricity price fluctuations. The dynamic optimizations conducted thus far are reactive, in the sense that no preparatory control action takes place prior to the change (demand or electricity price) being introduced. The preemptive case will be investigated in future studies.

A. Steady-state Optimization

The steady-state optimization is intended to obtain the desired operating points under the new scenarios. The decision variables used in this case are four degrees of freedom as described previously:

- liquid nitrogen production rate (F_{LN_2})
- fraction of top tray vapor routed to the PHX ($r_{gas\ draw}$)
- volumetric flow rate of air feed ($\dot{V}_{feed,std}$)
- flow rate of liquid air feed to the column ($F_{liq\ air}$)

together with the rate of evaporation of liquid nitrogen (F_{evap}) for unmet demand.

The demand cases were solved with demand satisfaction constraints that force the total GN_2 produced to meet the demand and eliminate overproduction:

$$\text{Demand} \leq F_{\mathrm{GN}_2,prod} + F_{evap} \leq \text{Demand} + \varepsilon_d, \qquad (14)$$

where ε_d is a specified tolerance. For the price change case, the total production rate is not required to meet a particular demand, but is not allowed to decrease below 70% of a specified base case production rate:

$$0.7F_{prod,base} \leq F_{\mathrm{GN}_2,prod} + F_{evap} \qquad (15)$$

Results for a number of the steady-state case studies conducted are tabulated in Table I. Data in the table are reported as ratios to the optimized base case results; since the base case amount of evaporated liquid nitrogen is zero, the values of F_{evap} are reported as a percentage of the base case optimal gas nitrogen production rate. A scaled impurity of unity corresponds to the maximum impurity constraint in the nitrogen product, and a scaled F_{LN_2} value of unity corresponds to the lower bound.

TABLE I
STEADY-STATE OPTIMIZATION SCENARIOS*

	Optimized Demand				Optimized Price	
	0%	-20%	+10%	+20%	$2C_{comp}$	$4C_{comp}$
F_{LN2}	1.00	1.00	1.00	1.00	1.00	1.00
$r_{gas\ draw}$	1.00	0.90	1.00	1.01	1.00	1.00
$\dot{V}_{feed,std}$	1.00	0.89	1.10	1.13	1.13	0.89
$F_{liq\ air}$	1.00	1.22	0.86	0.47	0.47	1.17
F_{evap}	0	0	0	6.28	0	0
Impurity	1.00	0.50	1.00	1.00	1.00	1.00
$F_{GN2,prod}$	1.00	0.80	1.10	1.13	1.13	0.89
Φ_{ss}	1.00	0.73	1.12	0.95	0.41	-0.97

*Values are reported as ratios to reference values.

The results presented here are not guaranteed to be globally optimal due to the nonconvexity of the problem. However, while attempting to solve the problem, a number of different initial guesses were provided in each case to attempt to obtain solution points that are close to the global optima.

As shown in Table I, in the optimized cases, the liquid nitrogen (LN_2) production is at its lower bound as there is no revenue associated with it. Also, it is optimal to first utilize available plant capacity before evaporating pre-stored LN_2 to meet the demand. This is due to the higher cost of evaporation relative to the the price of the gas nitrogen (GN_2) product. In all optimized cases, except the -20% demand change scenario, the plant operates at the maximum allowable steady state impurity level. In the 20% demand increase case, the flooding constraint becomes active, limiting the amount of GN_2 that can be produced by the plant, and necessitating vaporization of pre-stored LN_2 to meet the required product demand. The optimal objective function is seen to decrease due to the high cost of vaporization. In the case of the -20% demand change, constraints on the distillation column do not limit the performance of the plant, but the surge constraint of the compressor becomes active. These results imply that the operating window of the plant is defined by the flooding constraint and the surge constraint when the feed flow rate is considered.

The electricity price cases show an interesting result in the trade-off between revenue from production and electricity price. When the electricity price increases by a factor of 2, the optimal policy is to operate at the plant capacity, defined by the flooding constraint. However, when the electricity

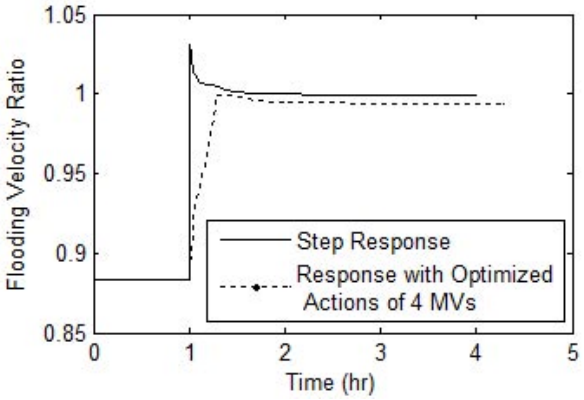

Fig. 2. Flooding velocity ratio at the critical tray.

price increases further, the plant production is reduced until the surge constraint of the compressor becomes active. At these electricity price levels, it is no longer beneficial to maximize production. We also observe in Table I that when the electricity price increases by a factor of four, the plant runs at a loss, which in practical terms is not sustainable.

B. Dynamic Optimization

Here, a dynamic optimization case study is conducted for the 20% demand increase case. Before applying dynamic optimization, a step test was performed to allow the plant to change from the optimal base case to the new operating point corresponding to the 20% demand increase case. Fig. 2 plots the ratio of gas velocity to the flooding velocity corresponding to the tray where this ratio is the largest. As can be seen, a direct step change is not desirable/applicable as it violates the flooding constraint during the transition. This provides an incentive for performing dynamic optimization.

The setup of the dynamic optimization is summarized in Table II. At $t = 1$ hr, the change in demand occurs. Recall that we implement piecewise linear control action. Decision variables in this case are slopes of the manipulated variables (see dynamic optimization formulation section), as well as the duration of each control interval. There are 5 control intervals in the problem, which gives a total of 25 decision variables. Fig. 3 presents the optimized trajectories for the 20% demand increase case. The flooding constraint is active, but not violated with the optimized control actions as was the case with the single step input. The optimal transition time of the inputs from the initial to the final steady-state operating point is 0.29 hrs.

As the flooding constraint limits the performance of the plant during transition for demand increase cases, it might

TABLE II
DYNAMIC OPTIMIZATION SETUP

	Duration Time	Decision Variable*
Initial	Fixed (1 hr)	Assigned to 0
Control‡	Optimized	Optimized
Settling	Fixed (3 hr)	Assigned to 0

*Slopes of the manipulated variables.
‡Include 5 Control Intervals.

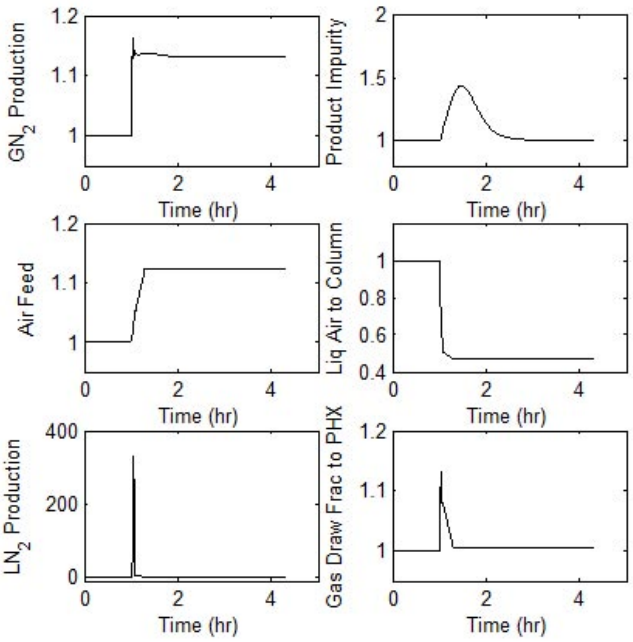

Fig. 3. Optimized trajectories of scaled variables for a positive 20 % demand change.

be beneficial to introduce the pre-stored LN_2 back to the column during a transition, without altering the tray design. The benefit of reintroducing stored liquid to air separation columns to reduce start-up times was demonstrated by Miller at al. [14]. Efforts are being undertaken to investigate this issue.

V. CONCLUSIONS AND FUTURE WORK

A. Conclusions

In this work, we present an optimization framework to investigate limits to fast transitions between operating points in a nitrogen plant. A dynamic model of a nitrogen plant was developed, with parameters adjusted using plant operating data. The optimization problem was formulated as a two tiered approach - steady-state optimization followed by subsequent dynamic optimization. It was found in the

steady-state optimization case studies that for the particular plant used, the lower and upper bounds of the operating window are defined by the compressor surge constraint and the flooding constraint. It was also found that there is a break point when the electricity price increases, at which point it is no longer beneficial to maximize production. A single step in the manipulated variables could result in constraint violation during transition, which motivates the necessity for performing constrained dynamic optimization. It was shown that with the optimized control actions, the system is able to effect transitions successfully without constraint violation. Another significant advantage of the approach is that it is independent of the configuration of the control system of the plant; the resulting transition trajectories thus represent a best-case scenario and can serve as a benchmark for any controller implementation.

B. Future Work

The potential benefit of introducing pre-stored LN_2 back to the column during transitions without altering the tray design for cases that require an increase in the air feed flow rate will be explored. In some cases, when the change in demand or electricity price is known in advance, reacting before the change actually affects the plant (i.e. preemptive action) may provide additional degrees of freedom to reduce the transition speed. A further avenue for investigation is to allow varying set-points for holdups in the reboiler and the sump to potentially improve the plant's agility/switchability.

VI. ACKNOWLEDGMENTS

The authors gratefully acknowledge support from the McMaster Advanced Control Consortium and Praxair, Inc.

REFERENCES

[1] M. Morari, "Design of resilient processing plants - III. A general framework for the assessment of dynamic resilience," *Chem. Eng. Sci.*, vol. 38, pp. 1881-1891, 1983.

[2] M. Morari and J.D. Perkins, "Design for Operations," in *Foundations of Computer-Aided Process Design*, L.T. Biegler and M.F. Doherty (Eds). AIChE Symposium Series, no. 304, vol. 91, CACHE-AIChE, pp. 1881-1891, 1995.

[3] J.M.G. van Schijndel and E.N. Pistikopoulos, "Towards the integration of process design, process control & process operability. Current status & future trends," in *Foundations of Computer-Aided Process Design*, M. Malone, J. Trainham and B. Carnahan (Eds.), American Institute of Chemical Engineers, 99-112, 2000.

[4] Y. Cao, D. Biss and J.D. Perkins, "Assessment of input-output controllability in the presence of control constraints," *Comp. Chem. Eng.*, vol. 20, no. 4, pp. 337-346, 1996.

[5] V. White, J.D.Perkins and D.M. Espie, "Switchability analysis," *Comp. Chem. Eng.*, vol. 20, pp. 469-474, 1996.

[6] C.L.E. Swartz, "A computational framework for dynamic operability assessment," *Comp. Chem. Eng.*, vol. 20, no. 4, pp. 365-371, 1996.

[7] L.T. Narraway and J.D. Perkins, "Selection of control structure based on economics," *Comp. Chem. Eng.*, vol. 20, pp. 469-474, 1996.

[8] M.J. Mohideen, J.D. Perkins and E.N. Pistikopoulos, "Optimal design of dynamic systems under uncertainty," *AIChE J.*, vol. 42, no. 8, pp. 2251-2272, 1996.

[9] R. Baker and C.L.E. Swartz, "Simultaneous solution strategies for inclusion of input saturation in the optimal design of dynamically operable plants," *Optimization and Engineering*, vol. 5, pp. 5-24, 2004.

[10] V. Sakizlis, J.D. Perkins and E.N. Pistikopoulos, "Recent advances in optimization-based simultaneous design and control," *Comp. Chem. Eng.*, vol. 28, pp. 2069-2086, 2004.

[11] S. Bian, M.A. Henson, P. Belaner and L. Megan, "Nonlinear state estimation and model predictive control of nitrogen purification columns," *Ind. Eng. Chem. Res.*, vol. 44, pp. 153-167, 2005.

[12] B. Roffel, B.H.L. Betlem and J.A.F. de Ruijter, "First principles dynamic modeling and multivariable control of a cryogenic distillation process," *Comp. Chem. Eng.*, vol. 24, pp. 111-123, 2000.

[13] V. Bansal, J.D. Perkins and E.N. Pistikopoulos, "A case study in simultaneous design and control using rigorous, mixed-integer dynamic optimization models," *Ind. Eng. Chem. Res.*, vol. 41, pp. 760-778, 2002.

[14] J. Miller, W.L. Luyben, P. Belanger, S. Blouin and L. Megan, "Improving agility of cryogenic air separation plants," *Ind. Eng. Chem. Res.*, vol. 47, pp. 394-404, 2008.

[15] G.J. Prokopakis and W.D. Seider, "Dynamic simulation of azeotropic distillation towers," *AIChE J.*, vol. 29, pp. 1017-1029, 1983.

[16] J.M. Smith, H.C. Van Ness, and M.M. Abbott, *Introduction to chemical engineering thermodynamics (7th ed.)*, McGRAW-HILL, NY; 2005.

[17] V. Bansal, R. Ross, J.D. Perkins and E.N. Pistikopoulos, "The interactions of design and control: Double-effect distillation," *J. Process Control*, vol. 10, pp. 219-227, 2000.

[18] M.J. Lockett, *Distillation Tray Fundamentals*, Cambridge University Press, NY; 1986.

[19] G.Y. Zhu, M.A. Henson and L. Megan, "Low-order dynamic modeling of cryogenic distillation columns based on nonlinear wave phenomenon," *Separation and Purification Technology*, vol. 24, pp. 467-487, 2001.

[20] Process System Enterprise Ltd, "Optimisation and Model Validation with gPROMS", 2009.

[21] Process System Enterprise Ltd, "gPROMS Introductory User Guide", 2004.